

Structure, optical properties and synthesis of Co-doped ZnO superstructures

Talaat M. Hammad · Jamil K. Salem ·
R. G. Harrison

Received: 1 February 2012 / Accepted: 29 February 2012 / Published online: 29 March 2012
© The Author(s) 2012. This article is published with open access at Springerlink.com

Abstract Co-doped ZnO nanoparticles were synthesized by a simple chemical method at low temperature with Co:Zn atomic ratio from 0 to 7 %. The synthesis process is based on the hydrolysis of zinc acetate dihydrate and cobalt acetate tetrahydrate heated under reflux to 65 °C using methanol as a solvent. X-ray diffraction analysis reveals that the Co-doped ZnO crystallizes in a wurtzite structure with crystal size of 12–5 nm. These nanocrystals self-aggregated themselves in a highly spherical superstructure of broad size distribution. High-resolution transmission electron microscopy image also shows that each sphere is made up of numerous nanocrystals with average interfringe distance of ~ 0.28 nm. The X-ray diffraction patterns, energy dispersive X-ray, scanning electron microscopy and high-resolution transmission electron microscopy micrographs of doping of Co in ZnO confirmed the formation of spherical superstructure and indicated that the Co^{2+} is successfully substituted into the ZnO host structure of the Zn^{2+} site. The optical band gap of ZnO nanoparticles was remarkably from 3.32 to 4.12 eV with increase of Co doping levels from 0 to 7 %. Photoluminescence measurements confirm these results.

Keywords Synthesis · Structural · Optical · Co-doped ZnO

Introduction

Zinc oxide (ZnO), being a wide-band-gap (3.3 eV) wurtzite-phase semiconductor, has attracted much attention here since some of the Zn can be substituted by magnetic transition metal (TM) ions to yield a metastable solid solution (Risbud et al. 2003; Bouloudenine et al. 2005; Thota et al. 2006). TM-doped ZnO has been theoretically proved to be one of the most promising materials for room-temperature ferromagnetism (Wang et al. 2006; Pearton et al. 2003). Zinc oxide is widely used in a number of applications like photocatalysis (Harbour and Hair 1979), gas sensors (Mitra et al. 1998), varistors (Gupta 1990), low-voltage phosphor material (Dijken et al. 2000) and so on. Recent prediction by Dietl et al. (2000) has increased the importance of transition metal-doped ZnO as a potential candidate in spintronics. Recent theoretical predictions (Sato and Katayama-Yoshida 2000; Hammad and Salem 2011) that transition metal (i.e., Mn, Co, Ni, V, Fe)-doped ZnO-diluted magnetic semiconductors (DMS) exhibit ferromagnetic properties at room temperature have led to increasing interest in further experimental studies of the material (Ueda et al. 2001; Lee et al. 2002; Pearton et al. 2007; Guillen et al. 2003; Schwartz et al. 2003). However, the origin of ferromagnetic behavior is not very well-known in these compounds. Recently, it was shown that the ferromagnetism in these materials can be induced by inclusions of nanoscale oxides of transition metals (Kittilstved et al. 2005) and/or nanoparticles containing a large concentration of magnetic ions (Sudakar et al. 2007). In many regards, Co^{2+} : ZnO is the archetypical dopant-sensitized wide-band gap semiconductor.

T. M. Hammad (✉)
Physics Department, Al-Azhar University,
P. O. Box 1277, Gaza, Palestine
e-mail: talaat@yahoo.com

J. K. Salem
Chemistry Department, Al-Azhar University,
P. O. Box 1277, Gaza, Palestine

R. G. Harrison
Department of Chemistry and Biochemistry,
Brigham Young University, Provo, UT 84602, USA

The visible photo-response of Co-doped ZnO has been observed by several researchers using single crystals (Kanai 1968) or polycrystalline of Co^{2+} : ZnO prepared by pellet sintering (Fichou et al. 1985). Zhang et al. (2008) reported a template-free solvothermal method for the formation of transition-metal-doped zinc oxide spheres and hollow spheres. They found that the Co-doped ZnO hollow exhibited ferromagnetism at room temperature, whereas nickel-doped ZnO hollow spheres exhibited only weak ferromagnetism at 300 K. Bhattacharyya and Gedanken (2008) found that the size of ZnO nanocrystals varied with the variation in cobalt concentration. The observed ferromagnetism was intrinsic in nature and not due to any metallic Co segregation or any cobalt oxide phase formation. The Co-doped ZnO nanoparticles of about 5 nm in size were synthesized by Tao Liu et al. (2008). Their results show a good incorporation of cobalt ions into substitutional zinc sites in zinc oxide. Cho et al. (2002) found ferromagnetic behavior in (Co, Fe)-doped ZnO film grown by reactive magnetron co-sputtering, where the effects of a rapid thermal annealing under vacuum lead to an increase in the magnetization and T_C . Wei et al. (2006) have deposited Fe-doped ZnO ($\text{Zn}_{1-x}\text{Fe}_x\text{O}$, $x = 0-0.07$) films onto LiNbO3 substrate by magnetron sputtering and found that Fe substituted the Zn site in the 2^+ charge state when $x \leq 0.04$ leading to a strong ferromagnetism ($T_C \sim 400$ K). A further increase in the dopant atomic fraction up to 0.07 caused the precipitation of magnetite (Fe_3O_4), which was conducive to the increase in the magnetic moment of the material. More recently, Kamakar et al. (2007) produced nanocrystalline Fe-doped ZnO powders by a chemical pyrophoric reaction method.

In this work, we report the synthesis and characterization of Co-doped ZnO into spherical superstructure using non-basic simple method with particle size ~ 12 to ~ 5 nm, without the assistance of base, template and surfactant. In this work, we also report the changes in the structural, morphologies and optical properties of ZnO nanoparticles brought about successful doping with cobalt.

Experimental procedure

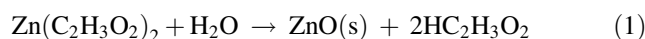
Zinc acetate dihydrate, $\text{Zn}(\text{Ac})_2 \cdot 2\text{H}_2\text{O}$ (99.9 %, Sigma Co.), cobalt acetate tetrahydrate, $\text{Co}(\text{Ac})_2 \cdot 4\text{H}_2\text{O}$ (99.9 % Sigma Co.) and methanol (99.9 % Sigma Co.) were used as received, without further purification. In a typical experiment, 2.195 g of $\text{Zn}(\text{Ac})_2 \cdot 2\text{H}_2\text{O}$ and the respective amount of $\text{Co}(\text{Ac})_2 \cdot 4\text{H}_2\text{O}$ were dissolved in 50 mL of methanol under vigorous stirring at room temperature and then ultrasonicated for 10 min. A clear transparent solution was obtained. The solution was heated at 65°C under reflux for 12 h. The precipitates were carefully collected and washed

with absolute ethanol several times to remove the ions possibly remaining in the final products, and then dried at 60°C for 2 h. A blue solid was obtained from the pink Co^{2+} solution.

The UV–vis absorption spectra of ethanolic nanoparticle solutions were recorded with Hewlett Packard 8453 spectrometer. The photoluminescence (PL) spectra measured at room temperature with a Perkin-Elmer LS 50B luminescence spectrometer and with a 320-nm excitation wavelength. Scanning electron microscopy (SEM) was performed with a Philips X130 ESEM-FEG with energy dispersive X-ray (EDAX) spectroscopy. The high-resolution transmission electron microscopy (HRTEM) analysis was done with a Tecnai F300 transmission electron microscope. Crystal structure identification and crystal size analysis were performed with an XDS 2000 X-ray diffractometer, (Scintac Inc., USA) with $\text{CuK}\alpha$ radiation source and scan rate of $2^\circ/\text{min}$.

Result and discussion

The pure and doped ZnO were synthesized by simply heating methanolic solutions of zinc acetate dihydrate. ZnO solid begins to form after about 8 h of heating and continues to form after the solution cools and sits at room temperature. The temperature of 65°C is critical to the formation of the materials. The water comes from zinc acetate dihydrate, supplies the oxide oxygen's and the acetates act as bases, thus no other base, such as hydroxide, is needed.



when the acetate salt of Co^{2+} was added to the zinc acetate solution during synthesis, ZnO precipitates again formed and the materials were no longer white.

Figure 1 shows the XRD patterns of Co-doped ZnO samples. The XRD showed that all samples exhibited the single crystal of hexagonal wurtzite structure in correspondence with JCPDS database of card number 36-1451, without the appearance of any secondary phase, suggesting that Co^{2+} incorporated to the Zn^{+2} sites in the crystal. Cobalt ions introduced as dopants at levels below 7 % shift the diffraction peaks to higher angles, suggesting that the unit cell contracting to occupy the ions (see Fig. 1a–e), and the width broadens due to the formation of smaller average diameters as a result of increase in disorder on Co^{2+} . Interestingly, the relative intensity of the XRD peaks varied with the increase in Co concentration and also with respect to ZnO (a). In b, the increased intensity peak of (002), (110) whereas (002) being as the preferred direction and decreased the intensity peaks of (100) and (101). The (002) peak is strongest in c and all other peaks have decreased.

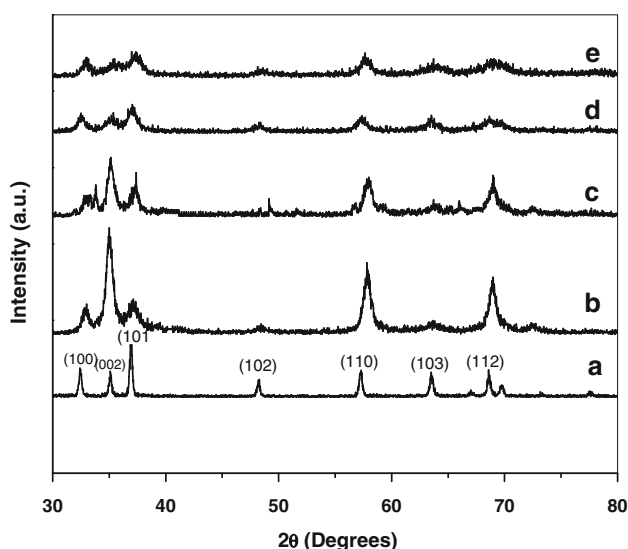


Fig. 1 a–e XRD patterns of Co-doped ZnO nanoparticles. **a** 0 %, **b** 1 %, **c** 3 %, **d** 5 % and **e** 7 % of Co

In d and e, the (101) peak is the strongest and (002) is decreased and being broader as compared with a. The interplay of XRD peaks intensities with the Co concentrations is only possible if Co^{2+} substitutes Zn^{2+} in the ZnO lattice to form Co-doped ZnO. Our XRD result is in good agreement with reported (Bhattacharyya and Gedanken 2008; Cui and Gibson 2005). The particle size D of the samples was determined using the Scherrer formula (Hammad et al. 2010):

$$D = \frac{k\lambda}{(B \cos \theta)}$$

where D is the particle size, k a fixed number of 0.9, λ the X-ray wavelength, θ the Bragg’s angle in radians, and B the full width at half maximum of the preferred peak in radians. The calculated average particle size of the Co-doped ZnO samples was found to be around 12–5 nm for Co doping concentration from 0 to 7 %. It seems that the particle size decreased with increasing the dopant concentration of cobalt. The percentages of Co in the doped ZnO samples (Table 1) were obtained by EDX analysis. The EDX data shows that the amount of Co incorporated into the ZnO matrix is less than the actual amount of dopants. Figure 2 depicts the energy-dispersive spectra (EDAX) of 7 % Co-doped ZnO. The spectra reveal that only three elements, Zn and O, and Co element exist in Co-doped ZnO nanoparticles.

Table 1 EDAX analysis of Co-doped ZnO samples

Element	Undoped	1 at. %	3 at. %	5 at. %	7 at. %	10 at. %
Co (%)	0	0.48	1.51	2.51	4.39	6.10
Zn (%)	99.80	99.52	98.49	97.49	95.61	93.90

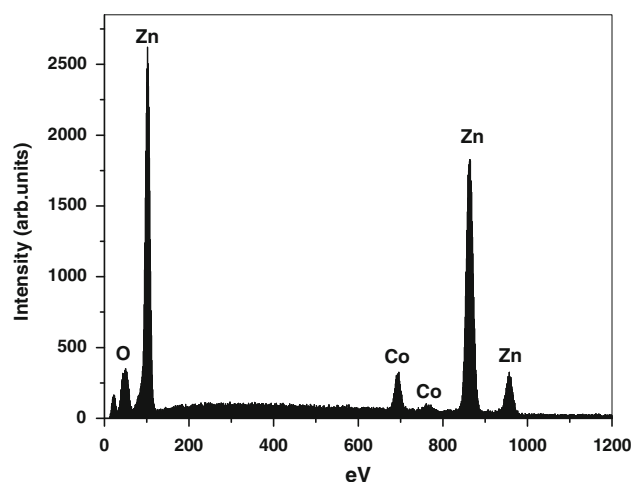


Fig. 2 EDAX spectrum percentage calculated of 7 % Co-doped ZnO nanoparticles

The morphology of the products was analyzed with SEM and high HRTEM. The SEM morphologies of pure and 7 % of Co-doped ZnO nanoparticles as synthesized are showed in Fig. 3a, b, respectively. The image showed a

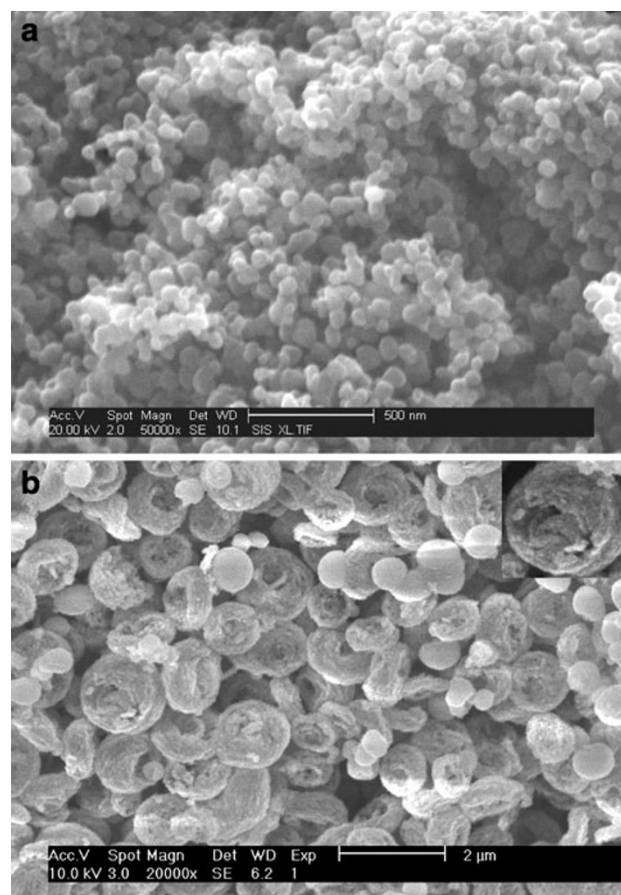


Fig. 3 SEM micrographs of Co-doped ZnO nanoparticles. **a** 0 % and **b** 7 % of Co

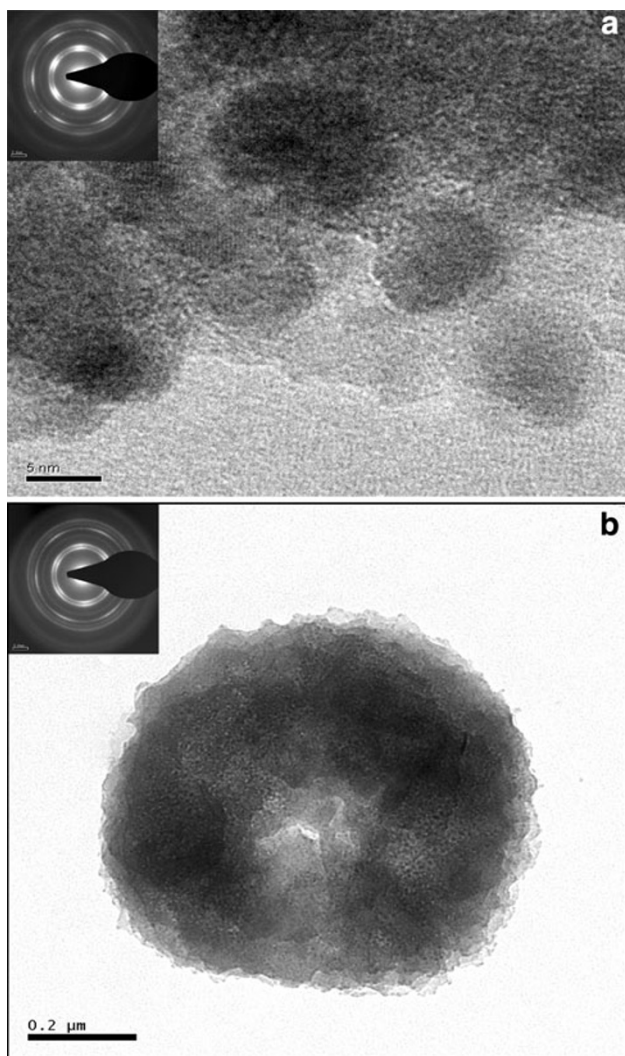


Fig. 4 a–c TEM micrographs of Co-doped ZnO nanoparticles. **a** 0 % and **b** 7 % of Co

nearly spherical nanoparticle with homogeneous size distribution of the ZnO nanocrystals is shown in Fig. 3a. Figure 3b presents the obtained spheres containing Co dopant of 7 %. It is seen from this figure that the growth of microspheres on Co doping. Moreover, the SEM indicates that the microspheres were porous with vacancies formed at their centers as shown in the inset of Fig. 2b. It is observed that the nanoparticles are self-aggregated in a closed-pack periodic array toward highly superstructure in size ranging from 600 to 1,300 nm. Figure 4 demonstrates HRTEM images taken for pure (Fig. 4a) and 7 % Co-doped ZnO nanoparticles (Fig. 4b) and corresponding selected area electron diffraction (SAED) patterns. It can be observed from the Fig. 4a that ZnO nanoparticles had a spherical morphology with an average diameter of 12 nm. From HRTEM micrographs, it is observed that Co-doped ZnO nanocrystals were self-aggregated toward porous spherical clustered nanoassemblies (superstructures) during the course of synthesis similar to the Mn-doped ZnO clustered assembly as discussed elsewhere (Barick and Bahadur 2007). Co-doped ZnO clustered nanoassembly is made up of three-dimensionally spatially connected numerous fine nanocrystals of size about 5 nm, which is in good agreement with the crystallite size obtained from XRD line broadening. The inset of Fig. 4 shows the bright field SAED patterns taken from different particles of pure and Co-doped ZnO (0–7 % of Co). These SAED patterns are indexed to the wurtzite ZnO structure, consistent with the above XRD results.

The results of HRTEM characterizations are shown in Fig. 5a, b. From HRTEM images, it is clearly observed that the average particle size of Co-doped ZnO nanoparticles was about 5 nm, which is consistent with the calculation results from XRD. It is also clear from HRTEM results that

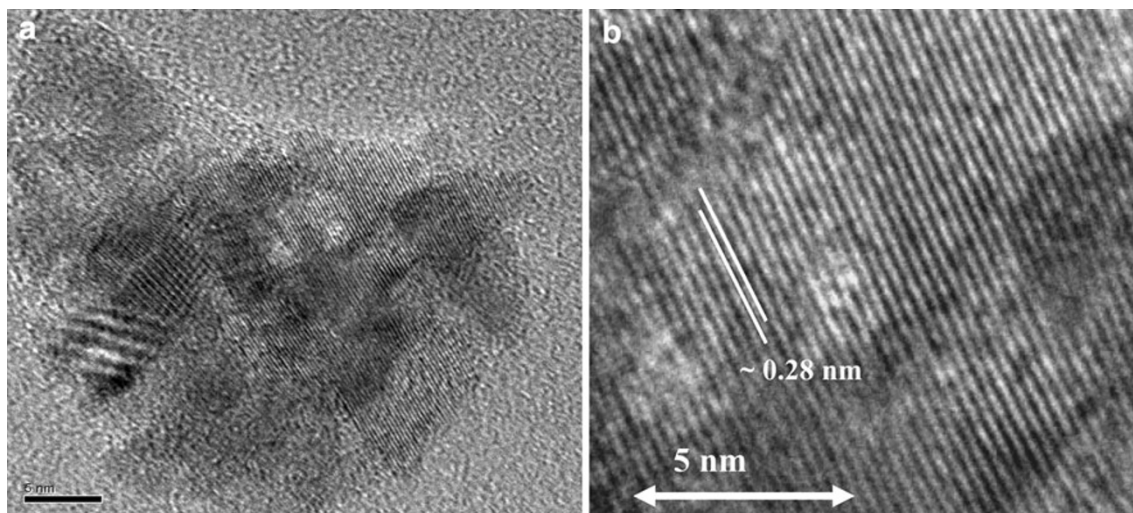


Fig. 5 a, b TEM micrographs of 7 % Co-doped ZnO nanoparticles

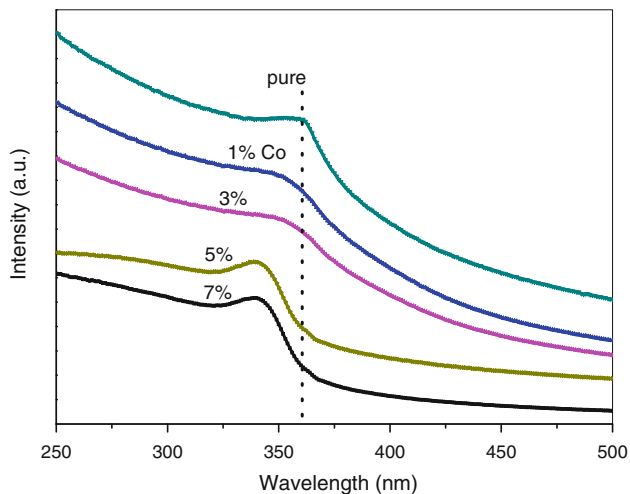


Fig. 6 UV-vis spectra of Co-doped ZnO nanoparticles at room temperature

Co doping in ZnO reduces the particle size. The average interfringe distance of co-doped ZnO nanocrystals was measured to be ~ 0.28 nm, which corresponds to the (002) planes of ZnO (Wang et al. 2008). According to the results of XRD pattern and HRTEM images, we believed that the Co ions were well incorporated into the crystal lattice of ZnO.

The optical properties of the Co-doped ZnO nanostructures were studied by UV-vis absorption spectroscopy. Figure 6 presents the typical absorption spectra of the pure and Co-doped ZnO nanoparticles with different levels of Co. Further, an obvious blueshift of the absorption edges can be observed in the doped ZnO samples from 361 to 340 nm of Co doping levels from 0 to 7 %. The band-gap energy (E_g) values for the samples were evaluated by plotting $(\alpha h\nu)^2$ versus $h\nu$ (Fig. 7) (Bahadur et al. 2010). The energy increases from 3.33 eV (pure ZnO) to 4.13 eV (7 % Co), and appears to originate from active transitions involving 3d levels in Co^{+2} ions and strong sp - d exchange interactions between the itinerant ‘ sp ’ carriers (band electrons) and the localized ‘ d ’ electrons of the dopant. It can be observed that Fig. 7 indicates a large blueshift of the band gap corresponding to samples of pure and 7 % Co-doped ZnO nanoparticles, respectively. The increase in the band gap or blueshift can be explained by the Burstein-Moss effect (Nirmala and Anukaliani 2011). This is the phenomenon that the Fermi level merges into the conduction band with an increase in the carrier concentration. Thus, the low energy transitions are blocked. Our results are in good agreement with the results reported by Sakai et al. (2006).

Figure 8 illustrates the photoluminescence spectra of the synthesized Co-doped ZnO nanoparticles with different doping concentration at room temperature. As shown in

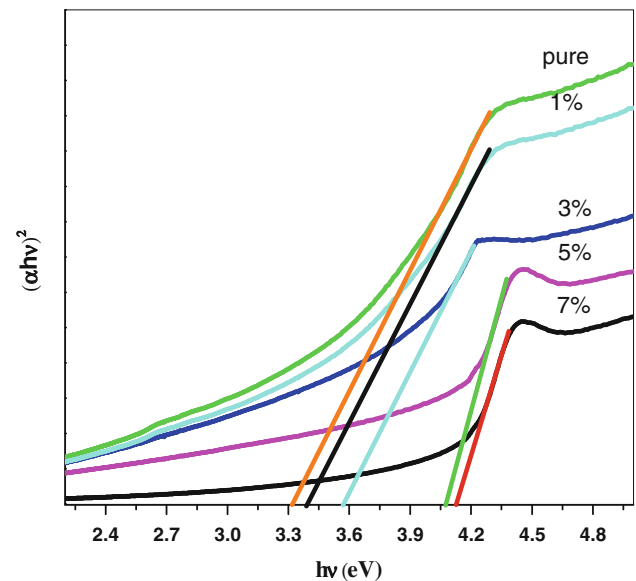


Fig. 7 Variation of band gap of Co-doped ZnO nanoparticles

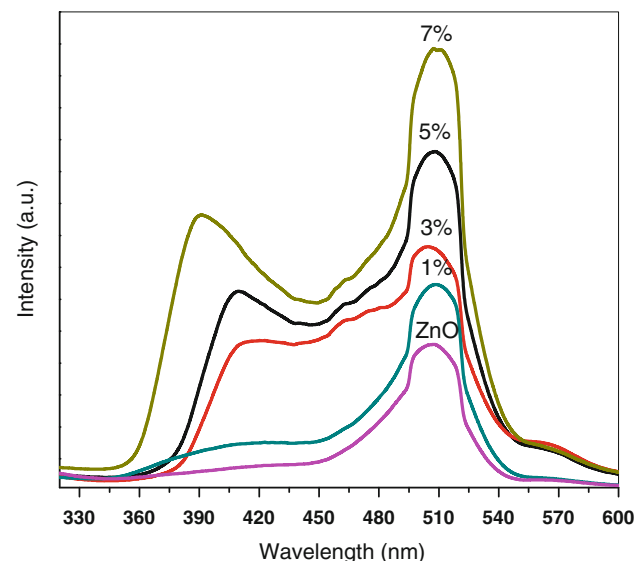


Fig. 8 a, b PL spectra of Co-doped ZnO nanoparticles at room temperature

Fig. 8, a weak ultraviolet (UV) emission at 405 nm and a very strong and broad green emission at 508 nm were observed for the pure ZnO nanoparticles. The UV emission at 405 nm is related to the near band-edge emission (Viswanatha et al. 2004), whereas the green is resulted from the recombination of electrons with holes trapped in singly ionized oxygen vacancies (Kong et al. 2001). Compared with the PL spectrum of pure ZnO, the UV-emission peak of Co-doped ZnO samples exhibits a large blueshift (from 410 to 390 nm); this is attributed to the shift of the optical band gap in these samples. A blueshift of the band

edge reveals the incorporation of Co in the lattice sites in ZnO. This supports the X-ray results on the incorporation of Co into the ZnO structure.

Conclusion

We have synthesized Co-doped ZnO nanoparticles by a simple chemical method at low temperature with Co:Zn atomic ratio from 0 to 7 %. The relative intensity of the XRD peaks varied with the increase in Co concentration with respect to ZnO nanoparticles. The average particle size of Co-doped ZnO was found 12–5 nm as calculated by XRD and transmission electron microscope (TEM). The XRD patterns, SEM and HRTEM micrographs of doping of Co in ZnO confirmed the formation of superstructure and indicated that the Co^{2+} is successfully substituted into the ZnO host structure of the Zn^{2+} site. The band-gap energy increases largely from 3.32 eV (pure ZnO) to 4.12 eV (7 % Co:ZnO), which is responsible for the blueshifts of wavelength in UV absorption and emission. Thus, the current doping method can be regarded as another effective technique to modulate the optical properties of ZnO nanoparticles.

Open Access This article is distributed under the terms of the Creative Commons Attribution License which permits any use, distribution, and reproduction in any medium, provided the original author(s) and the source are credited.

References

- Bahadur N, Srivastava AK, Kumar S, Deepa M, Nag B (2010) Influence of cobalt doping on the crystalline structure, optical and mechanical properties of ZnO thin films. *Thin Solid Films* 518:5257
- Barick KC, Bahadur DJ (2007) Synthesis, self-assembly, and properties of Mn doped ZnO nanoparticles. *J Nanosci Nanotechnol* 7:1935–1940
- Bhattacharyya S, Gedanken A (2008) Synthesis, characterization and room temperature ferromagnetism in cobalt-doped zinc oxide ($\text{ZnO}:\text{Co}^{2+}$) nanocrystals encapsulated in carbon. *J Phys Chem C* 112:4517
- Bouloudenine M, Viart N, Colis S, Kortus JD (2005) Antiferromagnetism in bulk $\text{Zn}_{1-x}\text{Co}_x\text{O}$ magnetic semiconductors prepared by the coprecipitation technique. *A Appl Phys Lett* 87:052501
- Cho YM, Choo WK, Kim H, Kim D, Ihm YE (2002) Effects of rapid thermal annealing on the ferromagnetic properties of sputtered $\text{Zn}_{1-x}(\text{Co}_{0.5}\text{Fe}_{0.5})_x\text{O}$ thin films. *Appl Phys Lett* 80:3358–3360
- Cui J, Gibson UJ (2005) Enhanced nucleation, growth rate, and dopant incorporation in ZnO nanowires. *J Phys Chem B* 109:22074
- Dietl T, Ohno H, Matsukura F, Cibert J, Ferrand D (2000) Zener model description of ferromagnetism in zinc-blende magnetic semiconductors. *Science* 287:1019–1022
- Dijken AV, Mulenkamp EA, Vanmaekelbergh D, Meijerink A (2000) Identification of the transition responsible for the visible emission in ZnO using quantum size effects. *J Lumin* 90:123
- Fichou D, Pouliquen J, Kossanyi J, Jakani M, Campet G, Claverie J (1985) Extension of the photoresponse of semiconducting zinc oxide electrodes by 3d-impurities absorbing in the visible region of the solar spectrum. *J Electroanal Chem* 188:167
- Guillen JMO, Johannsson B, Gehring GA (2003) Ferromagnetism above room temperature in bulk and transparent thin films of Mn-doped ZnO. *Nature Mater* 2:673
- Gupta TK (1990) Application of zinc oxide varistors. *J Am Ceram Soc* 73:1817
- Hammad TM, Salem JK (2011) Synthesis and characterization of Mg-doped ZnO hollow spheres. *J Nanopart Res* 13:2205
- Hammad T, Salem JK, Harrison RG (2010) The influence of annealing temperature on the structure, morphologies and optical properties of ZnO nanoparticles. *Superlattices Microstruct* 47:335–340
- Harbour JR, Hair ML (1979) Spin trapping; oxides; hydrogen peroxide; carboxyl radical ion; formate ion; peroxide. *J Phys Chem* 83:652
- Kanai Y (1968) Optical absorption and conduction due to Co^{2+} in ZnO crystals. *J Phys Soc Jpn* 24:956
- Karmakar D, Mandal SK, Kadam RM, Paulose PL, Rajarajan AK, Nath TK, Das AK, Dasgupta I (2007) Ferromagnetism in Fe-doped ZnO nanocrystals: experiment and theory. *Phys Rev B* 75:144404
- Kittilstved KR, Norberg NS, Gamelin DR (2005) Chemical manipulation of high- T_C ferromagnetism in ZnO diluted magnetic semiconductors. *Phys Rev Lett* 94:147–209
- Kong YC, Yu DP, Zhang B, Fang SQ, Feng W (2001) Ultra-violet emitting ZnO nanowires synthesized by a physical vapor deposition approach. *Appl Phys Lett* 78:407
- Lee HJ, Jeong SY, Cho CR, Park CH (2002) Study of diluted magnetic semiconductor: Co-doped ZnO. *Appl Phys Lett* 82:4020
- Liu T, Xu H, Chin WS, Yang P, Yong Z, Wee ATS (2008) Local structures of $\text{Zn}_{1-x}\text{TM}_x\text{O}$ (TM = Co, Mn, and Cu) nanoparticles studied by X-ray absorption fine structure spectroscopy and multiple scattering calculations. *J Phys Chem C* 112:13410–13418
- Mitra P, Chatterjee A, Maiti H (1998) ZnO thin film sensor. *Mater Lett* 35:33
- Nirmala M, Anukalini A (2011) Characterization of undoped and Co doped ZnO nanoparticles synthesized by DC thermal plasma method. *Physica B* 406:911–915
- Pearson SJ, Abernathy CR, Overberg ME, Thaler GT, Norton DP, Theodoropoulou N, Hebard AF, Park YD, Ren F, Kim J, Boatner LA (2003) Wide band gap ferromagnetic semiconductors and oxides. *J Appl Phys* 93:1
- Pearson SJ, Norton DP, Ivill MP, Hebard AF, Zavada JM, Chen WM, Irina AB (2007) ZnO doped with transition metal ions. *IEEE Trans Electron Devices* 54:1040
- Risbud AS, Spaldin NA, Chen ZQ, Stemmer SS (2003) Magnetism in polycrystalline cobalt-substituted zinc oxide. *R Phys Rev B* 68:205202
- Sakai K, Kakeno T, Ikari T, Shirakata S, Sakemi T, Awai K, Yamamoto T (2006) Defect centers and optical absorption edge of degenerated semiconductor ZnO thin films grown by a reactive plasma deposition by means of piezoelectric photothermal spectroscopy. *J Appl Phys* 99:043508
- Sato K, Katayama-Yoshida H (2000) Material design for transparent ferromagnets with ZnO-based magnetic semiconductors. *Japan J Appl Phys* 39:L555
- Schwartz DA, Norberg NS, Nguyen QP, Parker JM, Gamelin DR (2003) Magnetic quantum dots: synthesis, spectroscopy, and magnetism of Co^{2+} - and Ni^{2+} -doped ZnO nanocrystals. *J Am Chem Soc* 125(13):205
- Sudakar C, Thakur JS, Lawes G, Naik R, Naik VM (2007) Ferromagnetism induced by planar nanoscale CuO inclusions in Cu-doped ZnO thin films. *Phys Rev B* 75:054423

- Thota S, Dutta T, Kumar J (2006) On the sol–gel synthesis and thermal, structural, and magnetic studies of transition metal (Ni, Co., Mn) containing ZnO powders. *J Phys: Condens Matter* 18:2473
- Ueda K, Tabata H, Kawai T (2001) Magnetic and electric properties of transition-metal-doped ZnO films. *Appl Phys Lett* 79:988
- Viswanatha R, Sapra S, Gupta SS, Satpati B, Satyam PV, Dev BN, Sarma DD (2004) Synthesis and characterization of Mn doped ZnO nanocrystals. *J Phys Chem B* 108:6303
- Wang X, Xu J, Zhang B, Yu H, Wang J, Zhang X, Yu J, Li Q (2006) Signature of intrinsic high-temperature ferromagnetism in cobalt-doped zinc oxide nanocrystals. *Adv Mater* 18:2476
- Wang L, Chang L, Zhao B, Yuan Z, Shao G, Zheng W (2008) Systematic investigation on morphologies, forming mechanism, photocatalytic and photoluminescent properties of ZnO nanostructures constructed in ionic liquids. *Inorg Chem* 47:1443
- Wei XX, Song C, Geng KW, Zeng F, He B, Pan F (2006) Local Fe structure and ferromagnetism in Fe-doped ZnO films. *J Phys Condens Matter* 18:7471
- Zhang XL, Qiao R, Kim JC, Kang YS (2008) Inorganic cluster synthesis and characterization of transition-metal-doped ZnO hollow spheres. *Crystal Growth Design* 8:2609